ISSN 1063-7745, Crystallography Reports, 2008, Vol. 53, No. 7, pp. 1107–1111. © Pleiades Publishing, Inc., 2008.

STRUCTURE OF INORGANIC COMPOUNDS

Investigation of the Crystallization Features, Atomic Structure, and Microstructure of Chromium-Doped Monticellite

K. A. Subbotin[a], L. D. Iskhakova[b], E. V. Zharikov[a], and S. V. Lavrishchev[b]

[a] *A.M. Prokhorov General Physics Institute, Russian Academy of Sciences, ul. Vavilova 38, Moscow, 119991 Russia*

e-mail: soubbot@lsk.gpi.ru

[b] *Fiber Optics Research Center, Russian Academy of Sciences, ul. Vavilova 38, Moscow, 119991 Russia*

Received November 3, 2006

Abstract—A series of Cr^{4+}:$CaMgSiO_4$ single crystals is grown using floating zone melting, and their microstructure, composition, and crystal structure are investigated. It is shown that regions with inclusions of second phases, such as forsterite, akermanite, MgO, and $Ca_4Mg_2Si_3O_{12}$, can form over the length of the sample. The composition of the single-phase regions of the single crystals varies from the stoichiometric monticellite $CaMgSiO_4$ to the solid solution $Ca_{(1-x)}Mg_{(1+x)}SiO_4$ ($x = 0.22$). The Cr:$(Ca_{0.88}Mg_{0.12})MgSiO_4$ crystal is studied using X-ray diffraction. It is revealed that, in this case, the olivine-like orthorhombic crystal lattice is distorted to the monoclinic lattice with the parameters $a = 6.3574(5)$ Å, $b = 4.8164(4)$ Å, $c = 11.0387(8)$ Å, $\beta = 90.30(1)°$, $Z = 4$, $V = 337.98$ Å^3, and space group $P2_1/c$. In the monoclinic lattice, the $M(1)$ position of the initial olivine structure is split into two nonequivalent positions with the center of symmetry, which are occupied only by Mg^{2+} cations with the average length of the Mg–O bond $R_{av} = 2.128$ Å. The overstoichiometric Mg^{2+} cations partially replace Ca^{2+} cations (in the $M(2)$ position of the orthorhombic prastructure) with the average bond length of 2.347 Å in the [(Ca,Mg)–O_6] octahedron. The average distance in SiO_4 distorted tetrahedra is 1.541 Å.

PACS numbers: 81.10.–h, 61.72.–y, 66.66.Fn

DOI: 10.1134/S106377450807002X

INTRODUCTION

Chromium(4+)-doped monticellite (calcium magnesium orthosilicate) crystals compare favorably in their spectroscopic properties with many similar laser materials, including the known materials, such as forsterite and yttrium aluminum garnet [1–4]. However, no technology has been developed to grow monticellite single crystals of laser quality because of the incongruent melting of monticellite and the very narrow field of its primary crystallization in the $CaO–MgO–SiO_2$ system [5]. Only recently, Cr:$CaMgSiO_4$ single-phase samples of optical quality were prepared [6] and correct spectroscopic investigations of these crystals were performed [7]. It is also known that the crystallization process in the $CaO–MgO–SiO_2$ system near the $CaMgSiO_4$ stoichiometric composition results in the formation of $Ca_{1-x}Mg_xSiO_4$ solid solutions; as a result, the preparation of monticellite with a strictly stoichiometric composition is a complex problem [8]. According to [8, 9], the composition region of thermodynamically stable solid solutions lies between the $Ca_{0.89}Mg_{1.11}SiO_4$ and $Ca_{0.94}Mg_{1.06}SiO_4$ compositions.

In [9–11], the $Ca_{1-x}Mg_xSiO_4$ solid solutions were shown to be isostructural to forsterite Mg_2SiO_4 and the dependence of the metric of their orthorhombic lattice on the composition was investigated in detail. An X-ray diffraction study of monticellite crystals in the pressure range 0.001–60 kbar was performed in [12]. However, the distribution of cations over crystal lattice sites was not investigated by X-ray diffraction methods.

In this work, we investigated the specific features of the crystallization of monticellite from a melt, as well as the microstructure and composition of crystals under the conditions of their growth by crucible-free floating zone melting. The X-ray diffraction investigation of Cr^{4+}-doped monticellite crystals was carried out in order to reveal the geometric characteristics of structural polyhedra (necessary for the spectroscopic interpretation) and to determine the distribution of cations in the structure.

EXPERIMENTAL

Monticellite crystals were grown by crucible-free floating zone melting in air with optical heating on a URN-2-3P setup. Calcium carbonate (special-purity grade) preliminarily dried at a temperature of 120°C and magnesium and silicon oxides (special-purity grade) calcined at a temperature of 600°C served as the

initial reactants. Chromium(3+) oxide was used for doping samples by chromium. The chromium content in the initial charge was equal to 0.2 wt %. A mixture of the reactants was pressed into rods and sintered for 24 h at temperature of 1200°C. According to the data obtained in our earlier study [6], the optimum molar ratios $CaO:MgO:SiO_2$ of the components in the initial charge lie in the range from 32.7 : 31.7 : 35.7 to 33 : 31 : 36. The seeds used for the crystal growth were initially forsterite single crystals cut out along the *a* axis (*Pbnm* notation) and then monticellite crystals with the same orientation. The growth was performed in air. The pulling rate and the rotation rate of the upper (feed) and lower (receiving) rods were equal to 1 mm/h and 20 rpm, respectively. The rods were rotated in opposite directions, which provided a good mixing of the melt and a uniform optical heating of the melt zone.

The microstructure of the single-crystal samples was examined with a JSM-5910LV scanning electron microscope. The composition of the samples was determined using the energy-dispersive microprobe analysis. The crystal structure of the samples was determined by X-ray diffraction. The formed phases were identified and the parameters of their lattices were refined using the X-ray powder diffraction analysis (DRON 4-13 diffractometer, CuK_α radiation).

A single-crystal fragment ground to a nearly spherical shape (diameter, 0.15 mm) was used in the X-ray diffraction experiments. A set of experimental reflections was collected on a CAD4 diffractometer (MoK_α radiation; graphite monochromator; $\omega/2\theta$ scan mode; $0 \le \theta \le 75°$; $-7 \le h \le 7$, $0 \le k \le 6$, $0 \le l \le 13$). The experimental data were processed with the WinGX98 program package [13]. In solving the structure, two Mg atoms, by analogy with the $CaMgSiO_4$ structure [12], were placed at the inversion centers of the monoclinic lattice. The coordinates of the other atoms were located from a series of successive three-dimensional difference Fourier syntheses. The positional and thermal parameters of all atoms in the structure and the occupancies of the *M*(1) cation positions were refined by the full-matrix least-squares method in the isotropic approximation with the SHELX97 program package [14] (absorption correction in the spherical approximation, 673 reflections with $I > 4\sigma(I)$, $R = 0.051$, $s = 1.090$).

Table 1. Results of the analysis of the chemical composition of the single crystals in different regions*

Region nos.	Element content, at %			
	Ca	Mg	Si	O
1	14.28	14.32	14.26	57.13
2	12.41	15.56	14.69	57.34
3	10.81	16.81	14.92	57.46
4	10.11	17.43	14.97	57.43
5		27.72	14.85	57.49

* The maximum error in the determination of the elements is equal to ±0.17% for calcium, magnesium, and silicon and ±0.34% for oxygen.

RESULTS AND DISCUSSION

A series of monticellite crystals 10–15 mm in length and 6–7 mm in diameter was grown using floating zone melting from charges of different compositions lying in the primary crystallization field of monticellite and its immediate vicinity [6]. The crystallization in the oxide system under investigation is very sensitive to the initial composition of the melt, which, in addition, undergoes a considerable evolution during the growth run. As was shown in our previous paper [6], the refractory phases MgO, $CaMgSi_2O_6$, $CaMgSi_3O_8$, and $Ca_2MgSi_2O_7$ can be formed as solid inclusions in the melt. Inclusions are absent in the melts with compositions that are shifted from the stoichiometric point and contain no less than 36 wt % SiO_2. The phase composition and the microstructure of the grown crystals vary along the axis of their growth. According to the X-ray powder diffraction data, inclusions of forsterite, akermanite $Ca_2MgSi_2O_7$, periclase MgO, and the phase of the composition identified as $Ca_4Mg_2Si_3O_{12}$ were observed in different boule regions depending on the composition of the initial charge [6].

As follows from the results of the microprobe analysis, the grown boules contain single-phase regions with a composition that, within the limits of experimental error, corresponds to the stoichiometric composition of monticellite $CaMgSiO_4$ (Table 1, region no. 1). However, in the majority of cases, the microprobe analysis revealed the formation of $Ca_{(1-x)}Mg_{(1+x)}SiO_4$ solid solutions, for which a number of compositions are presented in Table 1 (region nos. 2–4). The most magnesium-enriched composition corresponds to $Ca_{0.78}Mg_{1.22}SiO_4$. Therefore, the compositions of the solid solutions formed in the samples under investigation can lie outside the region of thermodynamically stable monticellite compositions determined in [8, 9].

It should be noted that, since the crystallization of the melt and subsequent cooling of the formed crystals to room temperature occur at a finite (although rather low) rate, the compositions of the prepared samples are not necessarily thermodynamically equilibrium and stable.

Forsterite Mg_2SiO_4 (Table 1, Fig. 1) is one of the most important second phases in defect regions of the grown boules. Furthermore, no other second phases, except for forsterite, are revealed in the samples grown from the charges with compositions containing less than 33 wt % CaO.

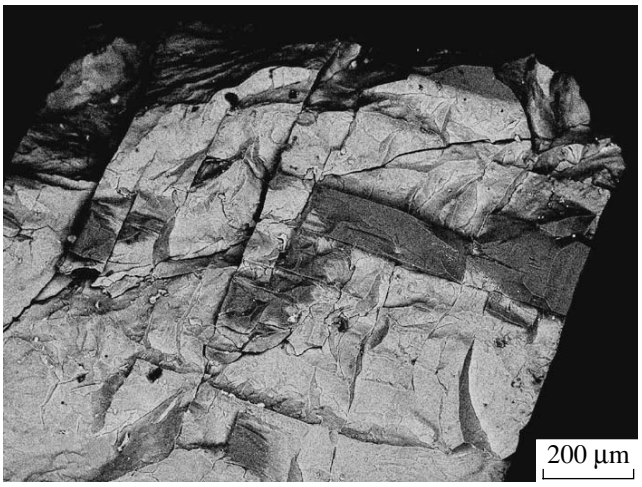

Fig. 1. Compositional contrast image of the monticellite crystal with forsterite inclusions (dark regions).

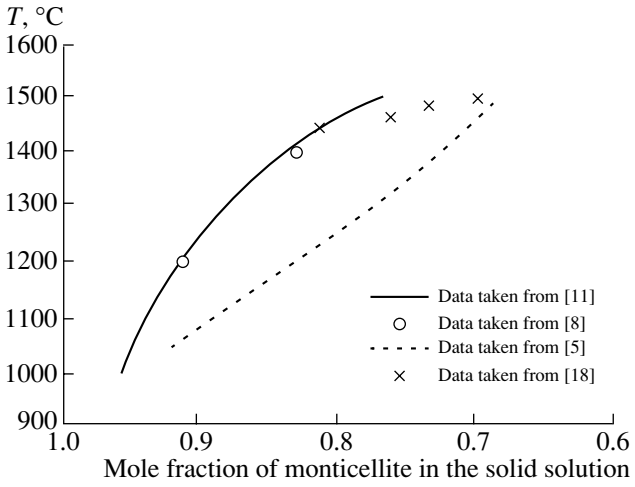

Fig. 2. Regions of the solid-phase solubility of forsterite in monticellite as a function of the temperature.

In our opinion, the monticellite–forsterite defect mixture is formed according to the following mechanism. At temperatures close to the melting point (approximately 1500°C), forsterite and monticellite form wide mutual-solubility regions (Fig. 2). However, cooling of the crystals after the growth leads to a sharp narrowing of the homogeneity regions. This results in the phase separation of solid solutions in the regions of the as-grown boules in which the value of x in the $Ca_{(1-x)}Mg_{(1+x)}SiO_4$ solid solutions exceeds a critical level. In this case, excess forsterite precipitates in the form of orthorhombic inclusions (according to the crystal system) up to several hundred microns in size (Fig. 1), which leads to the generation of high stresses and cracking of the crystal.

The above process can be observed visually: a transparent layer of the crystallized region is seen in the vicinity of the crystallization surface. However, the so-called cloud front associated with the intensive cracking and the precipitation of the second phase moves after the crystallization surface at a distance of several millimeters.

Table 2. Unit cell parameters of the crystals under investigation

Compound	a, Å	b, Å	c, Å	β, deg
$CaMgSiO_4$ [12]	4.821(2)	11.105(3)	6.381(1)	
$CaMgSiO_4$*	4.8135(6)	11.0063(19)	6.3259(11)	
$CaMgSiO_4$ [10]	4.8164	10.9869	6.3491	
Cr^{4+}:$Ca_{0.88}Mg_{0.12}SiO_4$*	6.3571(5)	4.8164(4)	11.0387(8)	90.30(1)
$Ca_{0.89}Mg_{0.11}SiO_4$ [9]	4.8180(6)	11.0074(9)	6.3327(6)	

* This study.

Table 3. Coordinates of atoms ($\times 10^4$) and their isotropic thermal parameters U_{eq} ($\times 10^4$, Å)

Atom	x/a	y/b	z/c	U_{eq}
M ($Ca_{0.88}Mg_{0.12}$)	0.7500(2)	0.0209(2)	0.72294(8)	0.00001
Mg(2)	0	0	0	0.00001
Mg(3)	0.5	0	0	0.00013(5)
Si	0.2497(2)	0.0887(2)	0.5822(1)	0.00001
O(1)	0.2501(5)	0.7547(7)	0.5782(2)	0.0008(7)
O(2)	0.2501(5)	0.2476(7)	0.4485(3)	0010(7)
O(3)	0.4562(5)	0.2281(7)	0.6486(3)	0028(7)
O(4)	0.0432(5)	0.2272(7)	0.6486(3)	0014(7)

Table 4. Bond lengths and angles in the Cr^{4+}:$Ca_{0.88}Mg_{0.12}MgSiO_4$ crystal structure

Bond	Length, Å	Bond	Length, Å
Mg1 octahedron		SiO_4 tetrahedron	
*M*1–O1 (×2)	2.183	Si–O_1	1.610
–O2 (×2)	2.083	–O_2	1.663
–O4 (×2)	2.118	–O_4	1.648
Average	2.128	–O_3	1.643
Mg1' octahedron		Average	1.641
*M*1'–O1 (×2)	2.188(3)		
–O2 (×2)	2.077(3)	Angle	Value, deg
–O3 (×2)	2.118(3)	O_1–Si–O_2	115.81
Average	2.128	O_1–Si–O_4	114.74
(Ca,Mg) octahedron		O_1–Si–O_3	114.80
M–O1	2.467	O_2–Si–O_4	102.31
–O2	2.293	O_2–Si–O_3	101.68
–O3	2.396	O_4–Si–O_3	105.85
–O4	2.270	Average	109.20
–O3'	2.268		
–O4'	2.392		
Average	2.347		

Note: Errors in the determination of the interatomic distances do not exceed 0.003 Å.

Table 5. Lifetimes of the $3T_2$ excited state of Cr^{4+} ions in crystals of the olivine series

Host crystal	Lifetime τ, μs		Ratio of the lifetimes at temperatures of 300 and 77 K	References
	300 K	77 K		
Mg_2SiO_4	2.7	25–35	8–11	[1, 2, 19]
Mg_2GeO_4	5	23	4.6	[2, 20]
$CaMgSiO_4$	5	16	3.2	[2]
	5.5	21	3.6	[4, 8]
γ-Ca_2SiO_4	15			[20]
γ-Ca_2GeO_4	15	25	1.7	[19, 21]

The X-ray diffraction investigations of the undoped crystals revealed that the single-crystal samples crystallize in the orthorhombic crystal system, whereas the symmetry of the lattice of the chromium-doped crystals is reduced from orthorhombic to monoclinic (space group $P2_1/c$, $Z = 4$ (Table 2)). It follows from the unit cell parameters refined from 25 high-angle reflections that the initial orthorhombic lattice is weakly distorted: the monoclinic angle β differs by only 0.29° from the right angle. The atomic coordinates are presented in Table 3. The selected interatomic distances and bond angles are given in Table 4.

According to the results obtained from the refinement of the occupancy of the cation positions in the structure, the crystal under investigation has the composition $(Ca_{0.88}Mg_{0.12})MgSiO_4$. As can be seen from Table 1, the unit cell parameters of the crystal are close to those calculated for the above composition according to the formulas derived by Lumpkin and Ribbe [10] with the use of the statistical treatment of the X-ray diffraction data obtained for 52 silicates, germanates, phosphates, and beryllates with an olivine structure.

In the compound under investigation, the *M*(1) positions in the olivine-type structure are occupied only by the magnesium cations. The average length of the Mg–O bond in these two inequivalent $[MgO_6]$ octahedra (Table 3) within the limits of experimental error coincides with the corresponding length $R_{av} = 2.133$ Å in the $CaMgSiO_4$ structure [12]. The overstoichiometric Mg cations replace some of the Ca cations in the *M*(2) positions of the initial prastructure. The average bond length in the $[(Ca,Mg)–O_6]$ octahedra is equal to 2.347 Å. A decrease in the distances in these polyhedra as compared to the distance of 2.370 Å in the $CaMgSiO_4$ structure [12] is caused by the partial replacement of the Ca^{2+} cations by the Mg^{2+} cations with a smaller ionic radius ($r_{Ca} = 1.00$ Å, $r_{Mg} = 0.72$ Å [15]). In the case where the symmetry of the lattice is reduced from orthorhombic to monoclinic with the loss of the *m* symmetry plane, the symmetry of the *M*(2) octahedra and XO_4 tetrahedra forming an olivine-type structure is changed to C_1. The distortion of the *M*(2) octahedron manifests itself in a large spread of its angles. The average distance in the SiO_4 tetrahedra increases insignificantly to 1.641 Å as compared to the corresponding distances of 1.625 Å in the $CaMgSiO_4$ structure [12] and 1.634 Å in the Mg_2SiO_4 forsterite structure [16].

The Cr^{4+} cations responsible for the laser properties of the crystal replace the silicon cations in the SiO_4 tetrahedra. The evaluation of the tetrahedron distortions from the coefficients relating the strains and symmetry of the tetrahedron [17] has demonstrated that the geometry of tetrahedra in the structures of the Cr^{4+}:$(Ca_{0.88}Mg_{0.12})MgSiO_4$ and $CaMgSiO_4$ [12] compounds does not undergo substantial changes. This explains the fact that the studied optical absorption spectra of the chromium-doped monticellite single-crystal samples grown from charges of different compositions and containing $Ca_{(1-x)}Mg_{(1+x)}SiO_4$ solid solutions with different compositions do not exhibit significant differences.

For crystals of the olivine series, there is a clear correlation between the atomic masses of the elements forming the host crystal and the lifetimes of the excited state of Cr^{4+} ions (Table 5). The data presented in Table 5 allow us to draw the conclusion that the lifetime τ is predominantly affected by the atomic mass of the diva-

lent ions of the host which are directly adjacent to the $[CrO_4]^{4-}$ cluster, whereas the atomic mass of the tetravalent ions has a weaker effect. In particular, a comparison of the fluorescence lifetimes for the γ-Ca_2SiO_4 and γ-Ca_2GeO_4 crystals at a temperature of 300 K has demonstrated that the replacement of silicon by germanium has almost no effect on this parameter.

The replacement of silicon by germanium in forsterite also has a considerably weaker effect on the thermal quenching as compared to the replacement of magnesium by calcium. In fact, the lifetime τ for the γ-Ca_2SiO_4:Cr crystal at a temperature of 300 K is longer than that for the γ-Mg_2GeO_4:Cr crystal by a factor of three. Even in the case of monticellite (i.e., upon replacement of only half the magnesium atoms by the calcium atoms) for which the value of τ is close to that for the Mg_2GeO_4 compound at 300 K, the decrease in the lifetime during heating from 77 to 300 K (the parameter more clearly characterizing the thermal quenching and, correspondingly, the decrease in the fluorescence quantum yield) for Mg_2GeO_4 is somewhat sharper than that observed for $CaMgSiO_4$ (Table 5).

Among the crystals compared in Table 5, the best spectroscopic characteristics are observed for the calcium silicate and calcium germanate, with the monticellite ranking next.

However, unlike monticellite, the γ-Ca_2SiO_4 and γ-Ca_2GeO_4 crystals cannot be grown using melt technologies because of the occurrence of subsolidus phase transformations. The use of complex and laborious flux technologies for growing γ-Ca_2GeO_4 crystals did not result in the preparation of single crystals comparable in quality to crystals grown from melt, including forsterite crystals. Attempts to grow γ-Ca_2SiO_4 single crystals have failed.

CONCLUSIONS

The results of our experiments on the growth of monticellite single crystals by using crucible-free floating zone melting with optical heating and the investigations of their properties will underlie the development of the technology used for synthesizing crystals of high laser quality.

ACKNOWLEDGMENTS

This study was supported by the Russian Foundation for Basic Research (project no. 08-02-01316).

REFERENCES

1. H. Eilers, U. Hommerich, S. M. Jacobsen, and W. M. Yen, Chem. Phys. Lett. **212**, 1092 (1993).
2. V. Petričevič, A. Seas, R. R. Alfano, et al., in *Advanced Solid State, Lasers, OSA Technical Digest, ATuE1 Abstract Paper* (The Optical Society of America, New Orleans, LU, United States, 1993), p. 238.
3. C. R. Pollock, D. B. Barber, J. L. Mass, and S. Markgraf, IEEE J. Sel. Top. Quantum Electon. **1**, 62 (1995).
4. K. A. Subbotin, E. V. Zharikov, V. A. Smirnov, and I. A. Shcherbakov, Kratk. Soobshch. Fiz., p. 16 (1997).
5. R. W. Ricker and E. F. Osborn, J. Am. Ceram. Soc. **37**, 133 (1954).
6. K. A. Subbotin, E. V. Zharikov, L. D. Iskhakova, and S. V. Lavrishchev, Kristallografiya **46** (6), 1115 (2001) [Crystallogr. Rep. **46** (6), 1030 (2001)].
7. T. F. Veremeĭchik, E. V. Zharikov, and K. A. Subbotin, Kristallografiya **48** (6), 1025 (2003) [Crystallogr. Rep. **48** (6), 974 (2003)].
8. G. M. Biggar and M. J. O'Hara, J. Am. Ceram. Soc. **52**, 249 (1969).
9. R. D. Warner and W. C. Luth, Am. Mineral. **58**, 998 (1973).
10. G. R. Lumpkin and P. H. Ribbe, Am. Mineral. **68**, 164 (1983).
11. G. E. Adams and F. C. Bishop, Am. Mineral. **70**, 714 (1973).
12. Z. D. Sharp, R. M. Hazen, and L. W. Figer, Am. Mineral. **87**, 748 (1987).
13. L. J. Farrugia, *WinGX98: X-Ray Crystallographic Programs for Windows* (University of Glasgow, Glasgow, United Kingdom, 1998).
14. G. M. Sheldrick, *SHELX97: Program for the Solution and Refinement of Crystal Structures* (University of Göttingen, Göttingen, Germany, 1997).
15. R. D. Shannon, Acta Crystallogr., Sect. A: Cryst. Phys., Diffr., Theor. Gen. Crystallogr. **32**, 751 (1976).
16. J. R. Smith and R. M. Hazen, Am. Mineral. **58**, 588 (1973).
17. G. Klebe and F. Weber, Acta Crystallogr., Sect. B: Struct. Sci. **50**, 50 (1994).
18. H. Y. Yang, Am. Mineral. **58**, 343 (1973).
19. V. Petričevič, A. B. Bykov, J. M. Evans, and R. R. Alfano, Opt. Lett. **21**, 1750 (1996).
20. L. Yang, V. Petričevič and R. R. Alfano, in *Novel Laser Sources and Applications*, Ed. by J. F. Becker, A. C. Tam, J. B. Gruber, and L. Lam (SPIE Optical Engineering, Bellingham, WA, United States, 1994); Proc. SPIE—Int. Soc. Opt. Eng. **PM16**, 103 (1994).
21. M. F. Hazenkamp, U. Oetliker, H. U. Güdel, et al., Chem. Phys. Lett. **233**, 466 (1995).

Translated by O. Borovik-Romanova